C. R. Geoscience 348 (2016) 510–519

Contents lists available at ScienceDirect

Comptes Rendus Geoscience

www.sciencedirect.com

Mathematical Geology

# Truncated Gaussian and derived methods

Hélène Beucher *, Didier Renard

*MINES ParisTech, PSL - Research University, Centre de géosciences, 35, rue Saint-Honoré, 77300 Fontainebleau, France*

ARTICLE INFO

*Article history:*
Received 15 July 2015
Accepted after revision 15 October 2015
Available online 8 March 2016

Handled by Sylvie Bourquin

*Keywords:*
Geostatistics
Categorical variable simulations
Truncated pluri-Gaussian
Sediment textures

ABSTRACT

The interest of a digital model to represent the geological characteristics of the field is well established. However, the way to obtain it is not straightforward because this translation is necessarily a simplification of the actual field. This paper describes a stochastic model called truncated Gaussian simulations (TGS), which distributes a collection of facies or lithotypes over an area of interest. This method is based on facies proportions, spatial distribution and relationships, which can be easily tuned to produce numerous different textures. Initially developed for ordered facies, this model has been extended to complex organizations, where facies are not sequentially ordered. This method called pluri-Gaussian simulation (PGS) considers several Gaussian random functions, which can be correlated. PGS can produce a large variety of lithotype setups, as illustrated by several examples such as oriented deposits or high frequency layering.


## 1. Introduction

The conversion of the geological characteristics of a field into a digital model is necessary to perform analyses such as scheduling the exploitation of a mine or detecting the pollution in a sedimentary environment. This conversion can be performed in two main different manners: either by understanding and mimicking the sedimentary processes (genetic models) or by directly reproducing the current facies arrangement resulting from several sedimentary and transformation processes (stochastic models).

The genetic models are the most efficient way to reproduce realistic sedimentation textures as they are based on physical processes (Cojan et al., 2005), but they require the precise knowledge of the whole set of processes that have led to the studied deposit. Moreover, honoring exactly the information provided by the data is still challenging (conditioning step). On the contrary, for stochastic models which are based on the resulting actual deposit image, the conditioning step is usually tractable. Different stochastic models are classically used; in those methods the texture characteristics are provided either in the training image for the multipoint simulation (MPS) (Mariethoz et al., 2010; Strebelle, 2002) or through the multivariable stochastic model for the sequential indicator simulation (SIS) (Alabert, 1987; Emery, 2004) and the truncated Gaussian model (TGS) (Matheron et al., 1987). With the latter TGS method, it is easy to define a lot of different multivariate models and hence to produce a large variety of arrangements with different relationships between facies.

The basic ingredients of TGS consist in the proportions of the facies and their spatial distribution and relationships. Initially the truncated Gaussian model has been introduced for reproducing a simple organization of ordered lithotypes. The lithotypes are then obtained by thresholding a single underlying Gaussian random function (GRF). It suffices to split the total domain of variation

* Corresponding author.
*E-mail addresses:* helene.beucher@mines-paristech.fr (H. Beucher), didier.renard@mines-paristech.fr (D. Renard).

http://dx.doi.org/10.1016/j.crte.2015.10.004

of the GRF in intervals and to assign each interval to a lithotype. The bounds of the interval (or the thresholds of the underlying GRF) are calculated so as to match the proportions of the various lithotypes. Finally the spatial characteristics of the GRF are related to those of the lithotype indicators which are described by their experimental variograms.

When the lithotype organization is more complex, in particular not sequentially ordered, it is necessary to consider several GRFs (hence the method called pluri-Gaussian, PGS). In that case, each lithotype is defined by its thresholds along each GRF. The partition scheme of the different GRFs into lithotypes is described by a synthetic graph called the lithotype rule. Finally, if some lithotypes must present linked shapes, it is possible to introduce some dependency between the GRFs (correlating them for example).

This paper provides a detailed description of the truncated Gaussian simulations and their derived methods. By a series of examples, it illustrates the large variety of lithotype setups produced simply by varying the lithotype rule and/or using particular structures for the underlying GRFs.

## 2. Method description

The geological interpretation to be modeled is composed of different sets of interest which constitute a partition of the space. These sets are the qualitative variables (lithotypes or facies in this paper) to be reproduced.

### 2.1. Qualitative properties

In order to perform calculations with qualitative properties it is necessary to transform them into numerical values beforehand. This can be done using the indicator function: the indicator of a given lithotype is equal to 1 when the observed point belongs to this lithotype and 0 otherwise. There are as many indicators as there are lithotypes involved in the deposit description, which turns the qualitative properties into a multivariable numerical setup. Moreover, as the indicators are numerical variables, it is now possible to consider their spatial characteristics through traditional tools such as simple and cross-variograms. The indicator variogram measures the probability that two points do not belong to the same lithotype (Eq. 1) as a function of their distance:

$$\gamma_B(h) = 0.5[P(x \in B, (x+h) \notin B) + P(x \notin B, (x+h) \in B)] \quad (1)$$

where $B$ is a lithotype, $P$ a probability, $x$ a point in the field, and $h$ the distance between point $x$ and another point in the field.

The indicator cross-variogram measures the probability that two points belong to two different lithotypes (Eq. 2) as a function of their distance:

$$\begin{aligned}\gamma_{AB}(h) &= 0.5E[(I_A(x+h)-I_A(x))(I_B(x+h)-I_B(x))] \\ &= -0.5[P(x \in A, (x+h) \in B) + P(x \in B, (x+h) \in A)]\end{aligned} \quad (2)$$

where $A$ and $B$ are two lithotypes and $I$ their indicators, $E$ the means, $P$ a probability, $x$ a point in the field, and $h$ the distance between point $x$ and another point in the field.

As the lithotypes constitute a partition of the space, when the indicator of a given lithotype is equal to 1, the indicators of the other lithotypes are equal to 0. This leads to particular relationships relating simple and cross-variograms of the indicators.

For instance, in Fig. 1a, a simulation has been performed using an object based model (Boolean simulation): in a white background, elongated grey objects are overlaid by black circular objects. Fig. 1b represents the simple variogram of each indicator calculated in north–south

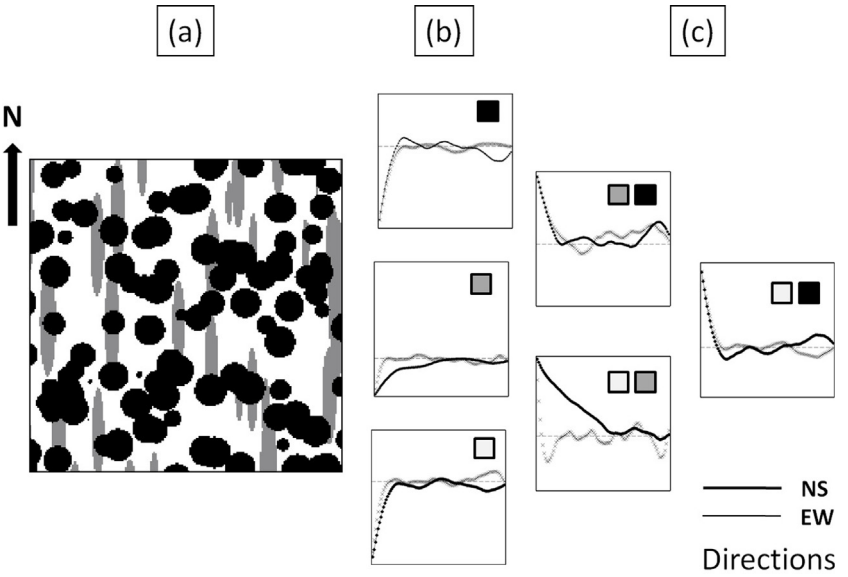


**Fig. 1.** On a simulated image in three sets (a), two directional variograms (NS and EW) are computed for each set (b: simple variograms) and for each pair of sets (c: cross-variograms).

and east–west directions, and the cross-variograms between any pair of indicators (Fig. 1c). The variogram of the black lithotype indicator is isotropic (same shape in all directions), while the variogram of the grey lithotype indicator is anisotropic: the dark curve (NS) stabilizes at a larger distance than the light curve (EW). The variogram of the white indicator is slightly anisotropic as complementary of the other two. The three cross-variograms (Fig. 1c) exhibit combinations of the different anisotropies. In order to produce a simulation that restitutes all these characteristics, it is important to use a consistent multivariate model that fits all these curves simultaneously.

### 2.2. Basic ingredients for the truncated Gaussian model

The truncated Gaussian model is an elegant solution for simulating a set of facies which corresponds to a consistent multivariate model for their indicator variables. All the lithotypes are obtained simultaneously from one normalized underlying GRF: they are simply obtained by thresholding this GRF (Armstrong et al., 2011).

The GRF displayed as a map (Fig. 2a1) is composed of values simulated according to a normal distribution (Fig. 2a2) and is characterized by its spatial structure (isotropic cubic model) summarized by its variogram (Fig. 2a3). In the truncated Gaussian framework, one interval on the GRF corresponds to a probability (hence a proportion) derived from the Gaussian cumulative density function. Conversely for a given proportion, the width of the interval (hence its bounds) depends upon the location of the interval along the cumulative density function. Fig. 2b and Fig. 2c represents two intervals for the black lithotype corresponding to the same proportion (∼18%). These two constructions are summarized in a diagram, the

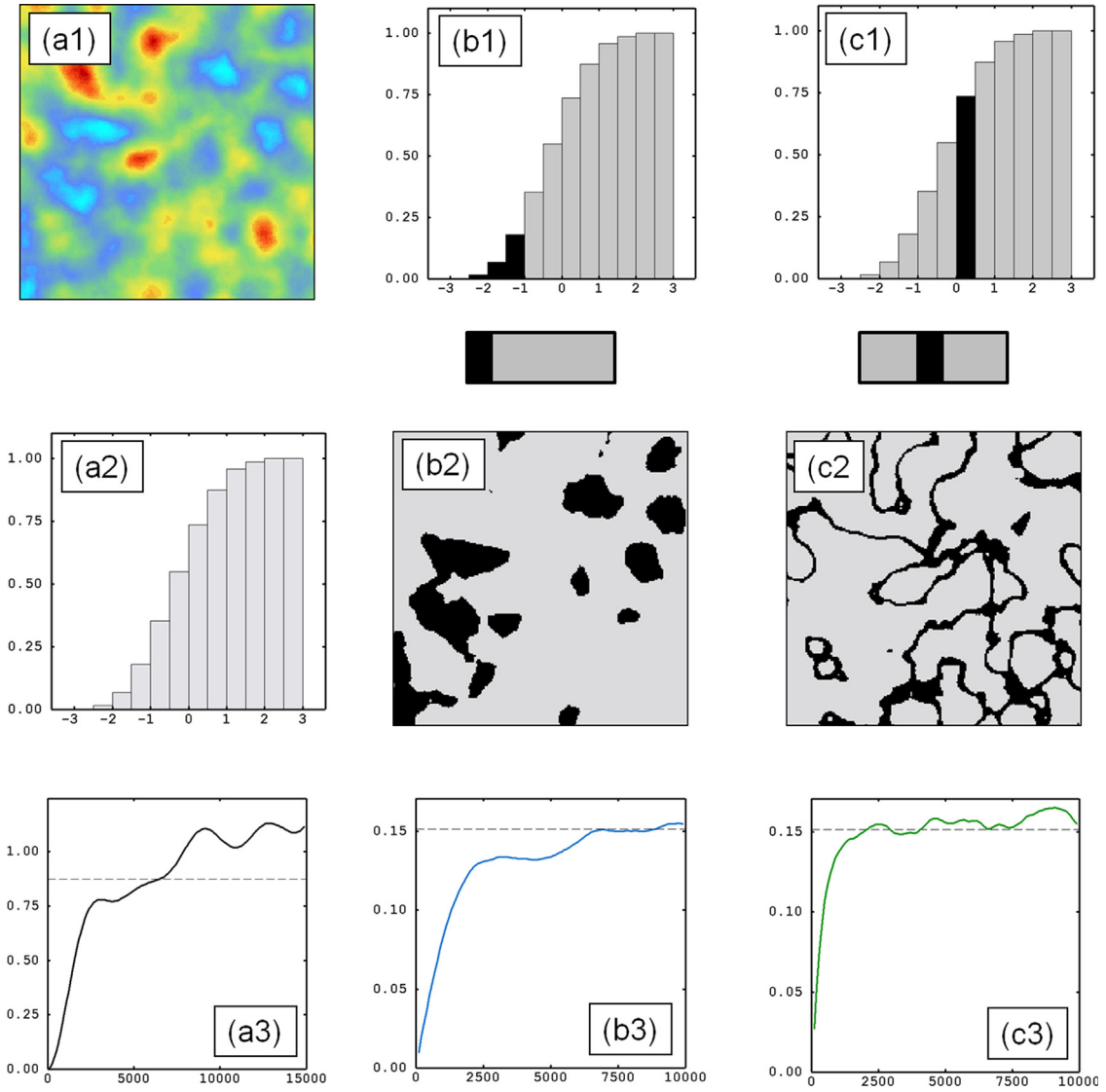


**Fig. 2.** A realization of a GRF according to an isotropic cubic model (a1), the corresponding cumulated density function (a2) and the experimental variogram (a3). A first lithotype rule (b1) leads to the lithotype simulation (b2) and its indicator variogram (b3). A second lithotype rule with an identical proportion (c1) leads to another lithotype simulation (c2) with its indicator variogram (c3).

lithotype rule (Fig. 2b1 and Fig. 2c1), where the Gaussian values are conventionally represented along the horizontal axis. The interval corresponding to the black lithotype is represented along this axis. Applying these two different thresholds to the same outcome of the GRF (as shown in Fig. 2a1) and with the same proportion, we obtain two black lithotype outcomes with different spatial structures: compact bodies for the first interval (Fig. 2b2) and elongated ones for the second one (Fig. 2c2).

This difference is also visible on the variograms of the indicators (Fig. 2b3 and Fig. 2c3) (the maximum distances for the variogram computation correspond to the quarter of the field size). An interval located close to the center of the Gaussian distribution leads to shorter range for the indicator variogram (Fig. 2c3) than when the interval concerns the lowest (or the largest) Gaussian values (Fig. 2b3): the lithotype changes at short distance are more frequent in Fig. 2c than in Fig. 2b. Conversely in Fig. 2c, the black lithotype exhibits clearly connected components longer than in Fig. 2b. It is important to underline that the variogram does not give information concerning the connectivity of the lithotypes. This characteristic that could be important for some studies can only be a consequence of the model. Connectivity used as an input constraint for lithotype simulations is still a difficulty. Several authors have proposed solutions for sequential algorithms, for instance in truncated methods (Allard, 1994) adding constraints in the simulation process, or in the multipoint approach (Renard et al., 2011) keeping only the multipoint configurations that satisfy the connectivity constraint.

The truncated methodology can be extended to represent several lithotypes ordered sequentially, with a single GRF. The lithotype rule describes the ordering of the lithotypes along the Gaussian cumulative density function, and dictates the neighboring relationships between

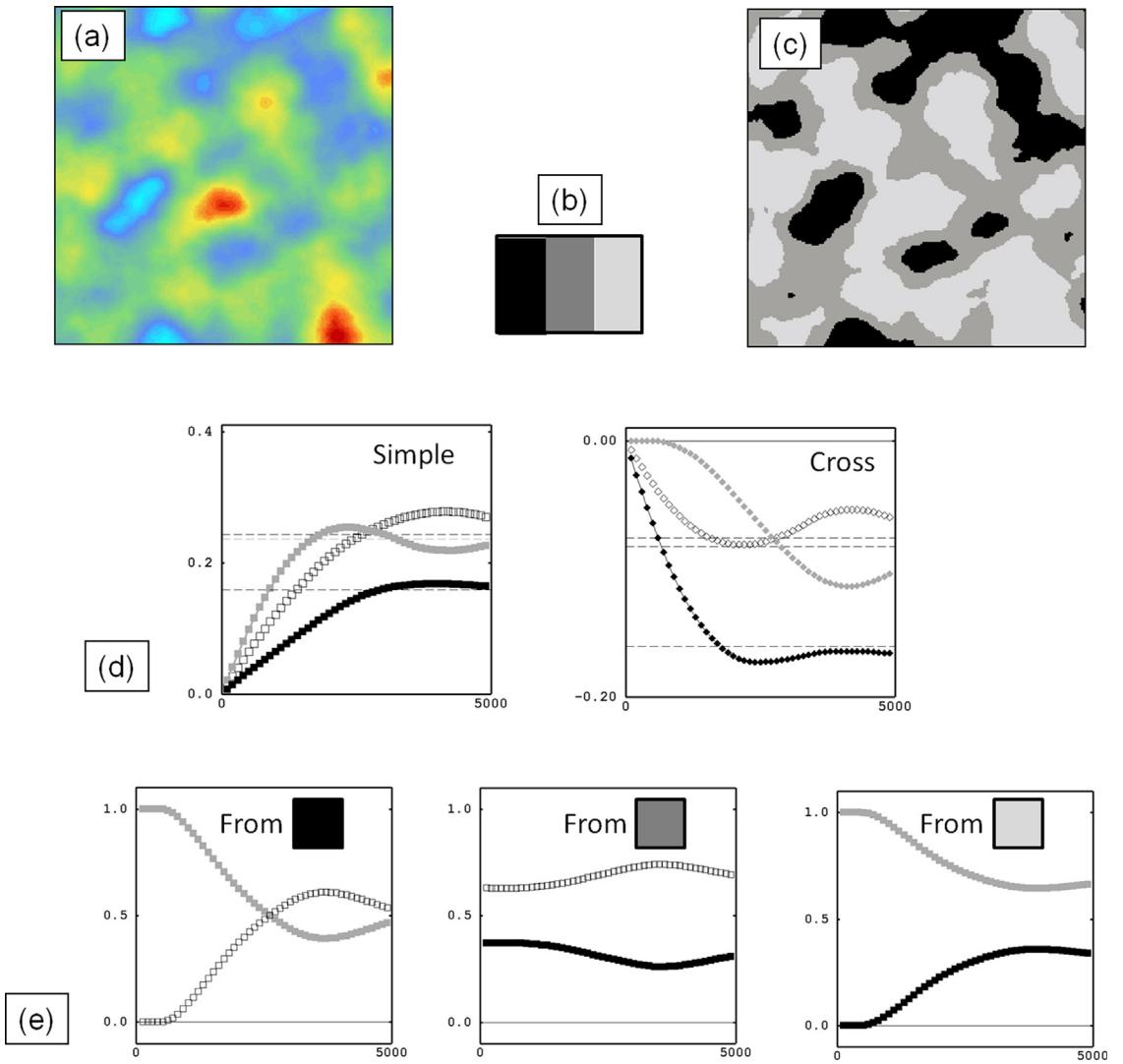


**Fig. 3.** Using the cubic GRF (a) and the lithotype rule (b), the indicator simulation (c) is obtained. The corresponding simple and cross-variograms whose color is the complementary color of the two lithotypes involved in the curve (d) characterize the lithotype arrangements, and the edge effect curves (e) quantify the contacts between them.

lithotypes. In Fig. 3a a GRF with an isotropic cubic model is considered. The lithotype rule (Fig. 3b) indicates that there should be no contact between black and light grey lithotypes, as demonstrated in the lithotype outcome (Fig. 3c).

The simple and cross-variograms of the three lithotypes are shown in Fig. 3d: they do not reproduce the cubic shape of the initial GRF. Note that because the GRF is isotropic each variogram is calculated without paying attention to the direction (omnidirectional). The sills of simple variograms depend on the lithotype proportions and the ranges depend on the Gaussian interval bounds: the intermediate lithotype (dark grey) has a shorter range than the others. The cross-variograms are all negative: as a matter of fact the lithotypes compose a partition of the space (at a given point only one indicator is equal to 1 the others being equal to 0), then the product of two terms non null is always negative (see Eq. 2). Another important remark for designing the lithotype rule is that the cross-variogram between the two lithotypes located at both extremities of the Gaussian axis (black and light grey) remains flat at short distances (equal to 0) as these lithotypes are not in contact.

As a conclusion, the spatial structures of the lithotypes described by their indicator variograms are linked to the spatial structure of the GRF (underlying variogram), but also involves the lithotype rule and the lithotype proportions. Note that some properties are transmitted from the spatial characteristics of the GRF to the lithotype indicator ones, such as anisotropy orientation. Moreover, unlike indicators for which the variogram models are specific, there is no limitation on the spatial characteristics of the GRF and then one can obtain very different multivariate indicator variogram models.

In order to choose the lithotype rule, other tools can be used to complete the analysis of the lithotype relationships: the edge effect functions (Eq. 3). These two-point statistics, function of their distance, give the probability that the first point $x$ belongs to a lithotype $A$ and the second point $(x + h)$ belongs to another lithotype $B$, where $h$ is the distance between the two points:

$$P[(x+h) \in B | x \in A, (x+h) \notin A] = \frac{-\gamma_{AB}(h)}{\gamma_A(h)} \quad (3)$$

On these edge effect curves (Fig. 3e), the ordering of the lithotypes are obvious. Starting from the black lithotype (left), the probability to be in light grey is null at small distance while the probability to be in dark grey is equal to 1. The same feature is visible when starting from the light grey lithotype (right) and entering in black or dark grey. When starting from the dark grey lithotype (middle) the probabilities are intermediate. For long distances, in a stationary case, all the curves tend to the probabilities ratio $P_B/(1-P_A)$.

The truncated Gaussian model with a single GRF produces layouts where lithotypes are ordered sequentially and presenting the same anisotropy. This method has been generalized by the use of two GRFs, leading to the pluri-Gaussian model (presented in supplementary figures S1, S2, S3). This improvement gives the opportunity to define different anisotropies for different lithotypes and to allow, or forbid, direct contacts between lithotypes. Then the resulting lithotype simulations go from nested to sequential lithotype arrangements.

### 2.3. In practice

In most studies, the available data is composed of wells scattered in a domain. The parameters which define the truncated Gaussian model are inferred from these data using the lithotype indicator functions. The lithotype rule is based on the geologist's knowledge ranging from the choice of the lithotypes (based on granulometry for instance) to depositional or transformation periods. The resulting construction is then validated with the simple and cross-variograms and the edge effect functions as explained in the previous section. Given the lithotype rule, the proportions of the lithotypes provide the intervals (thresholds) on the Gaussian values. Ultimately the simple and cross-variograms of the lithotype indicators define the model of the GRF(s).

The lithotype proportions are important ingredients of the method as the resulting simulations honor them. The proportions may vary in space. They are first computed along depth in order to check the vertical stationarity. The proportions of each lithotype are cumulated, from discretized information, along horizontal slices giving access to vertical cumulated proportions curves (VPC). These computations are performed with respect to a reference surface, i.e. within paleo-horizontal slices. Therefore a prior flattening may be necessary (Mallet, 2004; Perrin et al., 2012; Ramón et al., 2012). This flattening depends upon the analysis of the sequential stratigraphy (Ravenne, 2002) in consistency with the geological regional knowledge, in order to represent correctly the sequence of deposit which provides a typical signature on the proportions (Volpi et al., 1997).

It may also happen that the proportions show lateral variations. Then the lithotype proportions should be estimated on a 3D grid to account for a 3D non-stationarity of the lithotypes.

The estimation of the 3D lithotype proportions is a critical step. This estimation is performed either from lithotype indicators at wells or from vertical proportion curves. It can be constrained by auxiliary variables such as seismic attribute (Doligez et al., 2007) or using sequence stratigraphy concepts to define transition zones between wells (Labourdette et al., 2008). Finally this estimation is a challenging technique as the lithotype proportions are compositional variables (they must add up to 1).

## 3. Applications

The truncated Gaussian method allows the construction of a wide variety of lithotype relationships. This method has been successfully applied in various domains. In particular, Emery (2007) uses truncated Gaussian as a first step for estimating copper grades, Mariethoz et al. (2009) simulate heterogeneities in an aquifer to analyze fluid movements in a contaminated area, and Reverón et al. (2012) simulate the facies of unconsolidated sandstone oil

reservoir. The following examples (Figs. S1, S2, S3), extracted from different cases published in the literature, illustrate the adaptableness of the method to answer to more and more complex lithotype relationships. In the first case, the approach is classical with the use of a single underlying GRF and non-stationary lithotype proportions. The second case illustrates the use of correlated GRFs to reproduce linked facies shapes. The simulation of two linked indicators can also be obtained with associated pluri-Gaussian models as described in the third case. In the last three cases, variations in the lithotype rule and in the underlying GRF lead to specific textures, such as oriented facies or high frequency layering.

### 3.1. Sequential ordering

With a single GRF, the resulting simulation outcome corresponds to a deposit where the lithotypes are sequentially organized, for instance when lithotypes are assigned to classes with increasing clay contents.

This approach has been used to reproduce a turbiditic environment (Fig. 4). Vertical sections of an analog of an oil reservoir field have been sampled (Felletti, 2002, 2003). The first step of the study is to split the domain into sedimentary units, which will be simulated independently from each other. The top and bottom surfaces of each unit are mapped in a coherent way and reference grids for the proportion computations are chosen according to their geological environment. Fig. 4b represents the global vertical proportion curves of the different lithotypes: sand and mud with different characteristics (massive, laminated, etc.). In order to honor the lithotype non-stationarity, these proportions are estimated in the whole field from local VPCs. Finally the different units are simulated conditionally to the vertical sections and are merged together in order to construct the final realization of the field (Fig. 4c).

### 3.2. Non-tabular and interdependent deposits

The outcrop presented in Fig. 5a, located in Paradox Basin (Galli et al., 2006; Van Buchem et al., 2000), is the result of a submarine depositional sequence giving mainly horizontal structures and some algal mounds, which correspond to the vertical extensions visible on the geological interpretation (Fig. 5b). In the upper unit, the submarine structures follow the shape of the mounds.

To reproduce this complex deposit, where sets of lithotypes present different orientations and textures, two underlying GRFs are needed in the truncated pluri-Gaussian model. Moreover, the shape dependency is obtained by introducing a correlation between the two GRFs. The algal mound lithotypes (in green) and the surrounding marine lithotype (in yellow) are located in the lowest part of the lithotype rule and depend on the two GRFs (Fig. 5c). The vertical shape of the algal mounds and the smoothed contact between those lithotypes and the others are well reproduced on the conditional simulation (Fig. 5d).

### 3.3. Linked qualitative variables

When dealing with two qualitative variables, such as the sedimentology and the diagenesis index for example, several approaches can be considered (Doligez et al., 2010, 2011). One option consists in filling the unit with sedimentary lithotypes first using the most appropriate methodology, then simulating the diagenetic index with

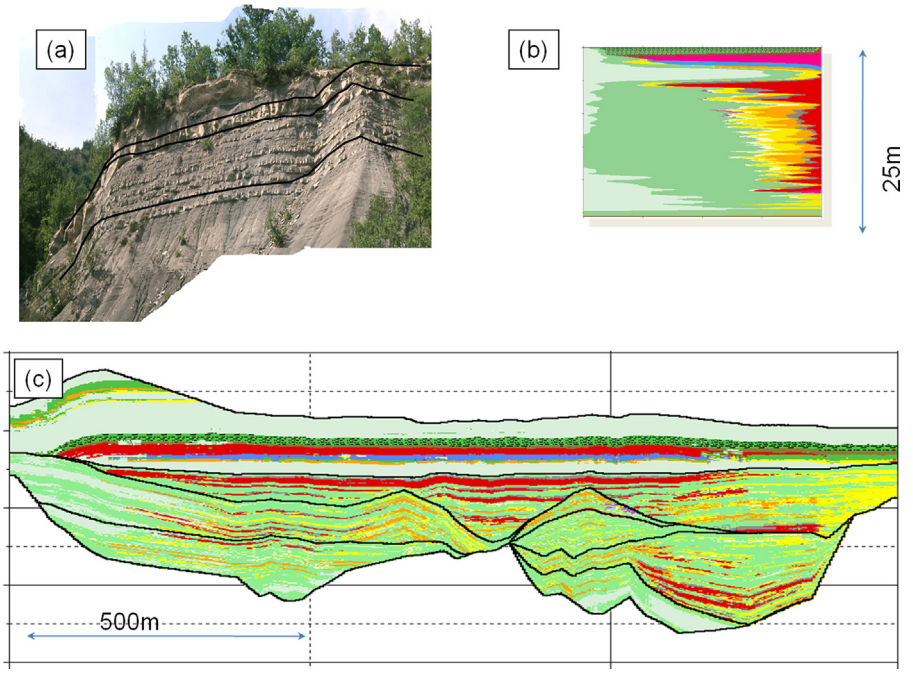


**Fig. 4.** Non-stationary simulation: part of the outcrop (a), global VPC (b) and conditional simulation (c) (Felletti, 2003).

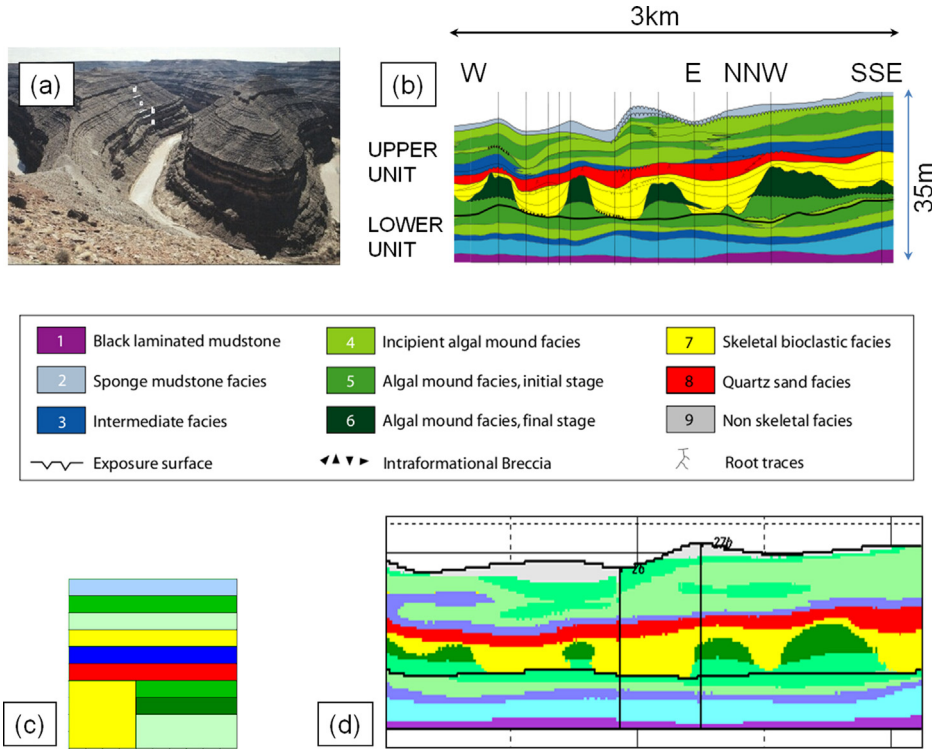


**Fig. 5.** Outcrop at Paradox basin (a), its geological interpretation (b), the lithotype rule for the upper unit (c) and a conditional simulation (d) (Galli et al., 2006).

the corresponding property per sedimentary lithotype. This sequential approach assumes independency of the diagenesis from one lithotype to another one (Fig. 6a).

Another possibility is to use the pluri-Gaussian method with a lithotype rule where the first GRF reproduces the organization of the sedimentary lithotype and the second GRF provides the sequence of the diagenesis indices (Fig. 6b). This approach allows to link the diagenesis index to the sedimentary facies, and to reproduce the gradual transitions for both variables. However, it assumes that each variable (sedimentation and diagenesis) presents an ordered organization as it is based on a single GRF.

A generalization which breaks this limitation is the use of two truncated pluri-Gaussian models, one for each phenomenon: hence the name of bi-pluri-Gaussian model (Renard et al., 2008). Then the layout of each phenomenon may be as complex as needed, i.e. two GRFs for each variable possibly correlated. Moreover, this model can honor a heterotopic data set: as a matter of fact, the diagenetic index is not necessarily measured at each sample where the sedimentary facies is known (Fig. 6c).

### 3.4. Particular shapes

The lithotype shapes can also be considered as resulting from a sedimentary process that induces some particular layouts. Some efforts have been carried out to reproduce these shapes using truncated Gaussian constructions, choosing appropriate underlying GRFs and/or lithotype

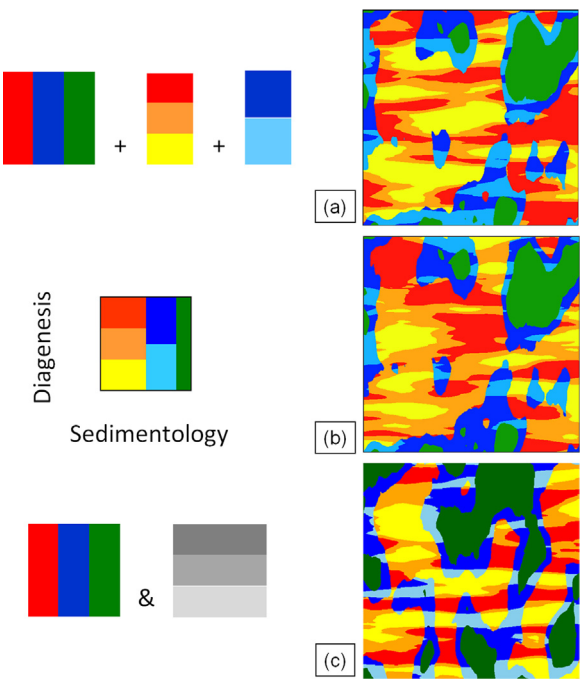


**Fig. 6.** Conditional simulations of two qualitative variables: sedimentology and diagenesis index. (a) sequential approach, (b) PGS, (c) Bi-PGS. Lithotype rules appear on the left of the associated simulations (Doligez et al., 2010).

rules. On the following simulations the aim is to reproduce particular shapes; they are not conditioned to any dataset.

As an example, one can obtain patterns similar to ripple marks on the beach (Fig. 7a) by using a GRF characterized by a periodic variogram (Fig. 7b), with the period being related to the wave dimension. The non-stationary density of ripples from top to bottom when water depth decreases is obtained by proportion changes (Fig. 7c).

Mixed scale textures can be reproduced using two underlying GRFs (Fig. 8a) and particular thresholding schemes. In these cases, a single facies can have variable sizes or orientations. In Fig. 8b, the black lithotype is ribbon shaped with large ribbons due to the GRF2 and thin at a smaller scale due to the GRF1. In Fig. 8c, the black lithotype is a mix with ribbon and grains depending on the thresholds.

### 3.5. Oriented shapes

Although the truncated pluri-Gaussian simulation method can generate complex layouts which cope with most of the sedimentary deposits, the outcomes always present a symmetrical pattern. Specific options have been designed to overcome this symmetry limitation and introduce an orientation in the facies organization.

This is the case when representing a uranium roll-front produced by the circulation of an oxidizing fluid in a fluvial deposit, where the mineralized zone is located at the forefront of the fluid penetration (Fig. 9a) (Langlais et al., 2008; Renard and Beucher, 2012).

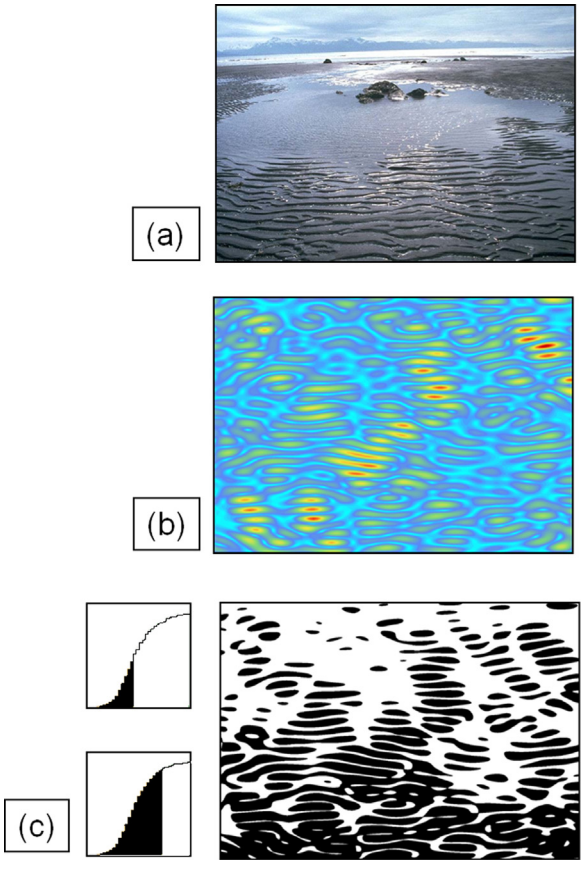


**Fig. 7.** Ripple marks (a), underlying GRF (b) and simulation (c).

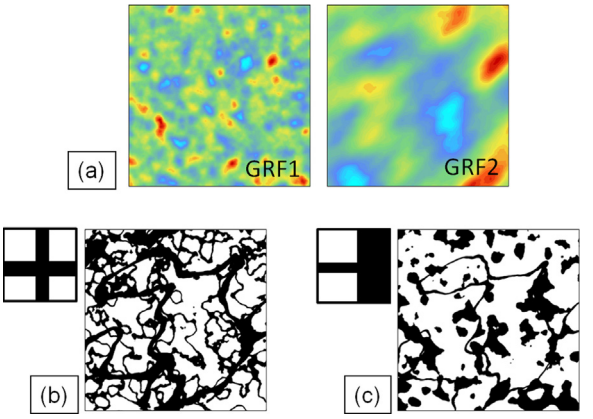


**Fig. 8.** Simulation of mixed scale textures: two GRFs with different ranges (a), a simulation with nested ribbon textures (b) and a mixed texture with ribbon and grains (c).

A solution consists in using two GRFs. The first one distributes oxidized versus reduced facies, and the second one locates the mineralized areas at the interface between the two phases while following the direction of the oxidizing fluid. It suffices to consider the second GRF equal to the first one shifted by a vector oriented along the flow direction and whose size is equal to the average dimension of the mineralized areas (Fig. 9b). Unfortunately this solution does not guarantee that the mineralized and the oxidized areas are contiguous. Moreover it leads to an equal size of the mineralized area over the whole field which may not be realistic.

The other solution starts from the same first GRF, but the mineralized area is obtained as the shadow cast by the

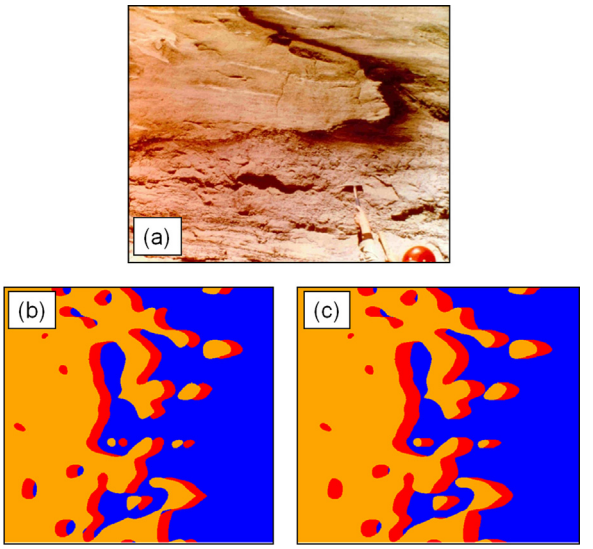


**Fig. 9.** Simulation of roll-fronts: outcrop photography (a), truncated Gaussian with translation (b) and shadow approach (c) (Langlais et al., 2008).

first GRF considered as a relief. The parameters of the light position and a possible truncation of the relief are deduced from the extension of the mineralized areas to be reproduced (Fig. 9c).

### 3.6. High-frequency changes

At a smaller scale (some centimeters), the facies organization may need to account for characteristics of high frequency transitions. For example, to reproduce ripples from marginal marine siliciclastic sediments (Fig. 10a) in sets of different properties (electric resistivity or rock hardness) a substitution model has been applied (Lantuéjoul, 2002). This model is similar to truncated Gaussian model: it corresponds to the coding of one GRF. However, in this model, the GRF has strictly stationary increments and the coding is a 1D simulation of a Markov chain process whose transition probability from one set to another is calibrated on the data (Fig. 10c). The length of the Markov chain is equal to the range of the simulated Gaussian values. On the resulting simulation, the anisotropy is determined by the GRF anisotropy and the lithotypes alternating depends on the transition probability between them (Fig. 10b).

By analogy, it is possible to construct a generalized truncated Gaussian, starting with a stationary underlying GRF, but using a lithotype rule simulated with a Markov chain. In that case the length of the Markov chain is chosen a priori. This construction allows reproducing other arrangements. For instance with a cubic model for the GRF and a cyclic Markov chain, the simulation result looks like a horizontal section in stromatolithes (Fig. 11).

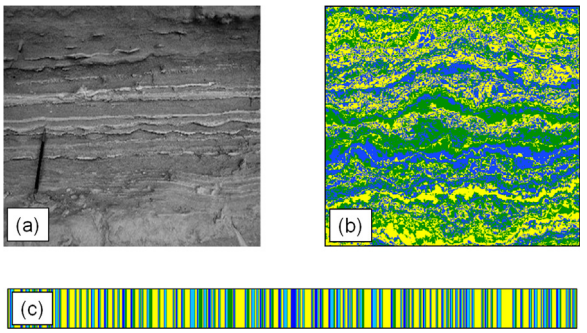


**Fig. 10.** Outcrop photograph of ripples (a), simulation from substitution model (b) and coding (c).

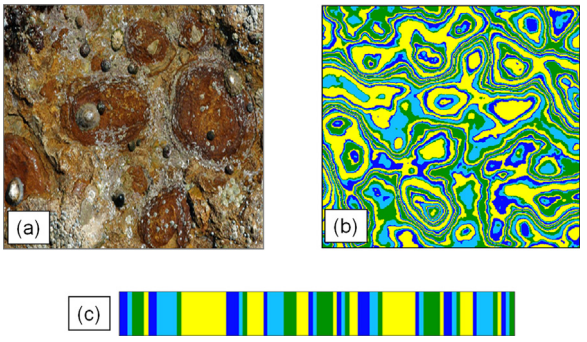


**Fig. 11.** Photograph of a horizontal section in a stromatolithe (a), simulation with generalized truncated Gaussian (b) and the simulated lithotype rule (c).

## 4. Conclusion and perspectives

As illustrated in the previous examples, the truncated Gaussian model and its derived methods give access to a wide variety of layouts. It can be used in a nested manner to simulate heterogeneities within bodies resulting from another genetic simulation. It can also jointly simulate a qualitative categorical variable (facies) and the corresponding continuous property (grade, porosity, etc.) while honoring the relationships between these two variables.

Due to its flexibility in accounting for additional constraints (quantitative or qualitative) added to its capability to condition the lithotype simulation to a set of data (even abundant), this truncated Gaussian model has been widely used for several studies. However the model is still evolving to answer to more and more complex lithotype arrangements, for instance the vertical dissymmetry of an oriented deposit sequence.

Other improvements concerning the parameter fitting are in progress. Because lithotype rule, proportions and variogram models are interdependent, their fitting could be delicate. Concerning the lithotype rule, Deutsch et al. (2014) and Astrakova and Dean (2014) propose new procedures to fit complex lithotype arrangements, using sequential and automatic procedures. For the GRF variogram fits, Desassis et al. (2014) have developed a methodology to compute the experimental variograms of the underlying GRFs starting from lithotypes at sample points and knowing the lithotype rule and the proportions; then the fit in a Gaussian framework is easier (stationary case and classical approach).

Finally, the latest challenge is to combine a physical model and a stochastic one to improve the lithotype simulations. The images would be more realistic as they are governed by physical equations and resort to the stochastic approach to account for the random part of the natural phenomenon.

## Acknowledgments

We are grateful to our colleagues who have developed the different extensions and experimented them in various case studies. We thank the invited editors for giving us the opportunity to submit our work in this special issue, and especially Pierre Weill who helped us in the revision process. We are indebted to Denis Allard (INRA) and another anonymous reviewer for their comments which improved the quality of this manuscript.

## Appendix A. Supplementary data

Supplementary material (Figs. S1, S2 and S3) associated with this article, can be found in the online version at: http://dx.doi.org/10.1016/j.crte.2015.10.004.

## References


Alabert, F., 1987. Stochastic imaging of spatial distributions using hard and soft information. Master's thesis, Department of Applied Earth Sciences, Stanford University, Stanford, 198 p.

Allard, D., 1994. Simulating a geological lithofacies with respect to connectivity information using the truncated Gaussian method. In: Armstrong, M., Dowd, P.A. (Eds.), Geostatistical Simulations. Kluwer Academic Publishers, pp. 197–211.

Armstrong, M., Galli, A., Beucher, H., Le Loc'h, G., Renard, D., Doligez, B., Eschard, R., Geffroy, F., 2011. PluriGaussian simulations in geosciences. Springer-Verlag, Berlin Heidelberg, 176 p.

Astrakova, A., Dean, S.O., 2014.In: Truncation map estimation for the truncated biGaussian model based on bivariate unit-lag probabilities, Proc. of EAGE 14th Eur. Conf. on the Mathematics of Oil Recovery.

Cojan, I., Fouche, O., Lopez, S., Rivoirard, S., 2005. Process-based reservoir modeling in the example of meandering channel. In: Leuangthond, O., Deutsch, C.V. (Eds.), Geostatistics Banff 2004, 1, Springer, The Netherlands, pp. 611–619.

Desassis, N., Renard, D., Beucher, H., Hamilton, S., Esterle, J., 2014. Experimental variogram of the underlying Gaussian random functions in the truncated pluri-Gaussian models. geoENV 2014.

Deutsch, J.L., Deutsch, C.V., 2014. A multidimensional scaling approach to enforce reproduction of transition probabilities in truncated pluri-Gaussian simulation. Stoch. Environ. Res. Risk Ass. 28, 707–716.

Doligez, B., Beucher, H., Lerat, O., Suza, O., 2007. Use of a seismic derived constraint: Different steps and joined uncertainties in the construction of a realistic geological model. Oil Gas Sci. Tech. Rev. IFP 62 (2), 237–248.

Doligez, B., Beucher, H., Pontiggia, M., Ortenzi, A., Mariani, A., 2010. In: Comparison of methodologies and geostatistical approaches for diagenesis quantification. AAPG Convention Article #40492, Denver, Colorado, USA, June 7-10, 2009.

Doligez, B., Hamon, Y., Barbier, M., Nader, F., Lerat, O., Beucher, H., 2011. In: Advanced workflows for joint modelling of sedimentological facies and diagenetic properties. Impact on reservoir quality. SPE paper 146621-MS, SPE Annual Tech. Conf. and Exhibition, 30 Oct.-2 Nov. 2011, Denver, Colorado, USA, 14 p.

Emery, X., 2004. Properties and limitations of sequential indicator simulation. Stoch. Environ. Res. Risk Ass. 18, 414–424.

Emery, X., 2007. Simulation of geological domains using the pluri-Gaussian model: New developments and computer programs. Comput. Geosci. 33, 1189–1201.

Felletti, F., 2002. Complex bedding geometries and facies associations of the turbiditic fill of a confined basin in a transpressive setting (Castagnola Fm., Tertiary Piedmont Basin, NW Italy). Sedimentology 49, 645–667.

Felletti, F., 2003. Statistical modelling and validation of correlation in turbidites: an example from the Tertiary Piedmont Basin (Castagnola Fm., northern Italy). Mar. Petrol. Geol. 21, 23–39.

Galli, A., Le Loc'h, G., Geoffroy, F., Eschard, R., 2006. An application of the truncated pluri-Gaussian method for modeling geology. In: Coburn, T.C., Yarus, J.M., Chambers, R.L. (Eds.), Stochastic modeling and geostatistics: principles, methods, and case studies, Volume II: AAPG Computer Applications in Geology 5, The American Association of Petroleum Geologists, pp. 109–122.

Labourdette, R., Hegre, J., Imbert, P., Insalaco, E., 2008. Reservoir-scale 3D sedimentary modelling: approaches to integrate sedimentology into a reservoir characterization workflow. Geol. Soc. London, Spec. Publ. 309, 75–85.

Langlais, V., Beucher, H., Renard, D., 2008. In the shade of the truncated Gaussian simulation. In: VIIIth Internat. Geostatistics Congress. 2, pp. 799–808.

Lantuéjoul, C., 2002. Geostatistical simulation: models and algorithms. Springer, Berlin, 256 p.

Mallet, J.L., 2004. Space-time mathematical framework for sedimentary geology. J. Math. Geol. 36 (1), 1–32.

Mariethoz, G., Renard, P., Cornaton, F., Jaquet, O., 2009. High-resolution truncated pluri-Gaussian simulations for the characterization of heterogeneous formations. Ground Water 47, 13–24.

Mariethoz, G., Renard, P., Straubhaar, J., 2010. The direct sampling method to perform multiple-point geostatistical simulations. Water Resour. Res. 46, W11536.

Matheron, G., Beucher, H., de Fouquet, C., Galli, A., Guérillot, D., Ravenne, C., 1987. Conditional simulation of the geometry of fluvio deltaic reservoirs. SPE 16753, 123–131.

Perrin, M., Poudret, M., Guiard, N., Schneider, S., 2012. Geological surface assemblage. In: Perrin, M., Rainaud, J.F. (Eds.), Shared earth modeling: Knowledge based solutions for building and managing subsurface structural models. Éditions TECHNIP, Paris, pp. 115–139.

Ramón, M.J., Pueyo, E.L., Briz, J.L., Pocoví, A., Ciria, J.C., 2012. Flexural unfolding of horizons using paleomagnetic vectors. J. Struct. Geol. 35, 28–39.

Ravenne, C., 2002. Sequence stratigraphy evolution since 1970. C. R. Palevol 1 (6), 415–438.

Renard, D., Beucher, H., Doligez, B., 2008. Heterotopic bi-categorical variables in pluri-Gaussian truncated simulation. VIII Int. Geostat. Congress, GEOSTATS 2008 1, 289–298.

Renard, D., Beucher, H., 2012. 3D representations of a uranium roll-front deposit. Appl. Earth Sci. 121 (2), 84–88.

Renard, P., Straubhaar, J., Caers, Mariethoz, G., 2011. Conditioning facies simulations with connectivity data. Math. Geosci. 43 (8), 879–903.

Reverón, J., Joseph, C., Doligez, B., Beucher, H., 2012.In: EAGE 2012 Copenhagen, Impact of microscopic heterogeneities of rock on elastic parameters in unconsolidated sandstones reservoir.

Strebelle, S., 2002. Conditional simulation of complex geological structures using multiple-point statistics. Math. Geol. 32 (1), 1–21.

Van Buchem, F., Doligez, B., Eschard, R., Lerat, O., Grammer, M., Ravenne, C., 2000.In: Stratigraphic architecture and stochastic reservoir simulation of a mixed carbonate/siliciclastic platform (Upper Carboniferous, Paradix Basin, USA), Elf Exploration Production F-64018 Pau.

Volpi, B., Galli, A., Ravenne, C., 1997. Vertical proportion curves: a qualitative and quantitative tool for reservoir characterization. Memorias del I Congreso Latinoamericano de Sedimentologia, Soc. Venezolana de Geol, Tomo 2, pp. 351–358.